










Output density quantification of electricity generation by flowing deionized water on graphene


Cite as: Appl. Phys. Lett. **117**, 123905 (2020); <https://doi.org/10.1063/5.0018862>

Submitted: 18 June 2020 . Accepted: 10 August 2020 . Published Online: 23 September 2020

Kei Kuriya, Kotaro Ochiai, Golap Kalita , Masaki Tanemura , Atsuki Komiya , Gota Kikugawa , Taku Ohara , Ichiro Yamashita, Fumio S. Ohuchi, M. Meyyappan , Seiji Samukawa , Katsuyoshi Washio, and Takeru Okada 

COLLECTIONS

 This paper was selected as Featured

 This paper was selected as Scilight



View Online



Export Citation



CrossMark

Lock-in Amplifiers
up to 600 MHz



Output density quantification of electricity generation by flowing deionized water on graphene

Cite as: Appl. Phys. Lett. **117**, 123905 (2020); doi: [10.1063/5.0018862](https://doi.org/10.1063/5.0018862)

Submitted: 18 June 2020 · Accepted: 10 August 2020 ·

Published Online: 23 September 2020



View Online



Export Citation



CrossMark

Kei Kuriya,¹ Kotaro Ochiai,¹ Golap Kalita,²  Masaki Tanemura,²  Atsuki Komiya,³  Gota Kikugawa,³  Taku Ohara,³  Ichiro Yamashita,⁴ Fumio S. Ohuchi,⁵ M. Meyyappan,⁶  Seiji Samukawa,^{3,7}  Katsuyoshi Washio,¹ and Takeru Okada^{1,a)} 

AFFILIATIONS

¹Department of Electronic Engineering, Tohoku University, Aoba 6-6-05, Aramaki, Sendai 980-8579, Japan

²Department of Physical Science and Engineering, Graduate School of Engineering, Nagoya Institute of Technology, Gokiso-cho, Showa-ku, Nagoya 466-8555, Japan

³Institute of Fluid Science, Tohoku University, 2-1-1 Katahira, Sendai 980-8579, Japan

⁴Graduate School of Engineering, Osaka University, 2-1 Yamadaoka, Suita, Osaka 565-0871, Japan

⁵Department of Materials Science and Engineering, University of Washington, Box 352120, Seattle, Washington 98195, USA

⁶NASA Ames Research Center, Moffett Field, California 94035, USA

⁷AIMR, Tohoku University, 2-1-1 Katahira, Sendai 980-8579, Japan

^{a)}Author to whom correspondence should be addressed: takeru.okada@tohoku.ac.jp

ABSTRACT

Energy conversion by water flowing over graphene is a promising mode of energy harvesting. However, the mechanism, energy-conversion efficiency, and quantification of power density for this mode of interfacial electricity generation remain unknown. Quantification of the output performance for the flow-induced electricity generation using graphene is presented in this work. The output performance per unit contact area between water and graphene is found to be proportional to the flow speed, with an electromotive force density of 0.0025 [$(\mu\text{V}/\text{mm}^2)/(\text{mm}/\text{s})$] for the conditions used in this work. The ability to quantify output density will help to construct guidelines for future applications of this form of electricity generation.

Published under license by AIP Publishing. <https://doi.org/10.1063/5.0018862>

The ever-increasing global energy demand requires the development of alternative modes of energy harvesting. Thus, next generation energy-conversion systems aim to combine off-the-grid devices with nano- and micro-based technologies to create feasible solutions. Among these, an energy-conversion system that utilizes carbon nano-materials and flowing liquid has great potential because of the abundance of natural bodies of water on the earth. Examples of interfacial electricity generation by liquid flow over carbon materials have been reported by several groups.^{1–7} However, the mechanisms proposed to describe the phenomena including momentum transfer,⁸ coulombic field-based theories,^{9–12} capacitive charge and discharge,¹³ and streaming potential^{14–17} are still under debate. Some studies consider this form of electricity generation a type of triboelectric nanogenerator,^{18–22} while others consider the role of specific solute ions in the

primary mechanism despite the fact that electricity can be generated on carbon materials by both de-ionized (DI) water and electrolyte solutions.

The lack of a definite mechanism makes the conversion efficiency of liquid flow over carbon materials difficult to define at the nano- and micro-scale. In turn, the lack of clear conversion efficiency makes decision-making regarding the practical utilization impossible, thus hindering the application potential. The total amount of energy generation is not a crucial problem in this system; once devices are deployed in an environment, the amount of generated energy is free from the device volume because the environment is regarded as an infinite energy reservoir. While the need for quantification of the energy generation is generally acknowledged as important, it has not been measured to date. Here, we report the results of our effort on the

quantification of electricity generation at the interface between graphene and flowing water. The electromotive force from water flow on graphene is defined by the average flow speed in a micro-channel and the contact area between graphene and water.

A glass plate used as a substrate has access ports for water and electrical connections. The plate was washed successively with acetone, ethanol, and DI water in a sonication bath. Pristine graphene was synthesized by low pressure chemical vapor deposition on copper foil using polystyrene as a carbon source.^{23,24} Graphene was transferred onto the substrate using poly-methyl-methacrylate (PMMA) as a sacrificial film. The PMMA film was removed by dipping in acetone overnight at room temperature. PMMA residue was then etched by annealing in a 3% hydrogen/argon mixture at 300 °C for 3 h. In the schematic in Fig. 1(a), a silicone spacer was sandwiched between the graphene on the substrate and the top plate. The height and width of the spacer, which give the cross section of the fluidic channel, are 300 and 3400 μm , respectively. Poly-tetra-fluoro-ethylene tubes were used for DI water supply, and the water flow was driven by suction using a syringe pump (YMC Corporation, YSP-201) to avoid leakage by applied pressure. Gold electrodes were used with an arbitrary distance d on graphene and connected to a digital multimeter (Keithley, DM7510) by coaxial cables through the electrical connecting ports at the top plate. The electrodes were located outside the fluidic channel to prevent contact with water. A tunable external load resistance was connected in series to the graphene, and a digital multimeter recorded the generated voltage between both ends of the load. The time interval between voltage measurements was every 20 ms. All measurements were made at room temperature in a space that was electrically

shielded. We used undoped pristine graphene in this study and no doping effects were considered.

The Raman spectrum measurement was carried out using a commercial micro-Raman system (JASCO, NRS-5100). A typical Raman spectrum of graphene on the substrate shown in Fig. 1(b) was taken using a 532-nm laser through a 100 \times objective lens. Three major peaks were observed at 1350, 1580, and 2700 cm^{-1} , which are assigned to the D-, G-, and G'-bands, respectively. The G'-band consists of a single component, and the intensity ratio of the G-band and G'-band indicates monolayer graphene.²⁵ The peak of the D-band originates from the transfer process. The typical electrical resistance of the graphene varied from 0.1 k Ω to several tens of k Ω .

The electrical property of graphene during water flow was investigated first. The electrical signals were measured at both ends of the graphene along the water-flow direction. A single pulse-like flow was applied for voltage generation. The generated voltage was observed just after flow started and followed the on/off switching [Fig. 2(a)]. Figure 2(b) shows that the resistance of graphene stays constant during the water-flow, indicating that the load resistance governs the output like a typical battery. The direction of the electrical current is always the same as that of the water flow.

Next, the cyclic response of the voltage generation was investigated. Figure 3(a) shows that the response is repeatable and reproducible, and the magnitude of the generated voltage depends on the flow speed. A delay in the signal response is observed under higher flow speed conditions, originating from the experimental setup. This delay may be caused by the shape change of the connecting components at higher water pressures or by the inertia of water in the microchannel. The external load resistance was tuned to maximize the output performance. Figure 3(b) indicates that the generated voltage approaches saturation at high load resistance, as expected. The electromotive force is obtained using the following equation:

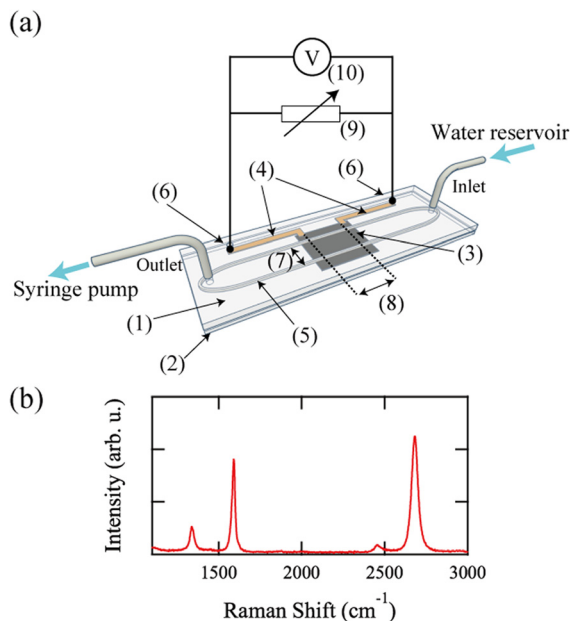


FIG. 1. (a) Schematic illustration of a micro-flow-chip with graphene. The flow chip consists of (1) glass top plate, (2) glass substrate, (3) graphene, (4) electrodes, (5) silicone spacer, (6) electrical connection ports, (7) channel width, (8) channel length: d , (9) load resistance, R_L , and (10) digital multimeter. (b) Typical Raman spectrum of graphene. The spot size of the laser is approximately 1 μm .

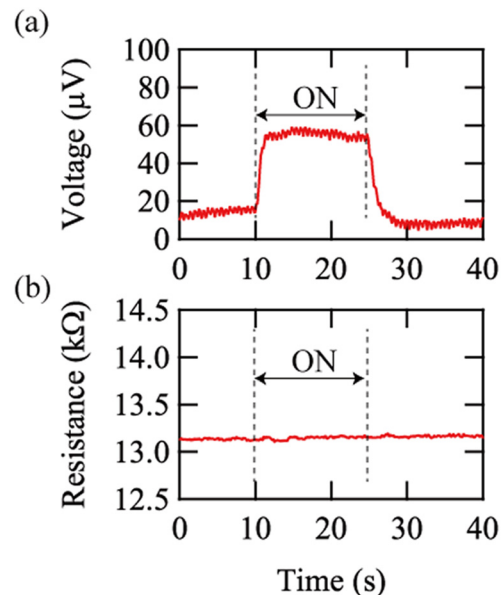


FIG. 2. (a) Generated voltage and (b) resistance of graphene. The channel length and flow speed are 3 mm and 245 mm/s, respectively.

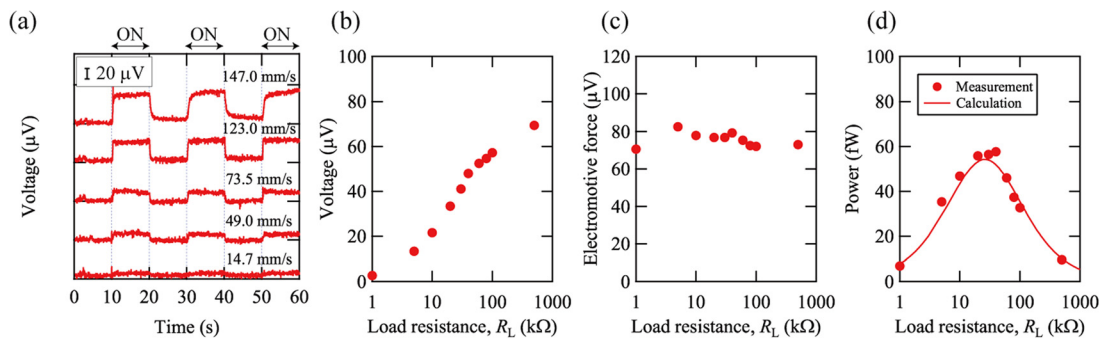


FIG. 3. Measurements of typical (a) voltage signal, (b) generated voltage, and (c) electromotive force. (d) Measured output power and calculation curve. The internal electric resistance of graphene is 26 kΩ in this case.

$$E = \frac{r + R_L}{R_L} V, \quad (1)$$

where E , V , r , and R_L are the electromotive force, generated voltage, electrical resistance of graphene, and external load resistance, respectively. Figure 3(c) indicates that the electromotive force remains nearly constant throughout the measurements with different load resistance values. Furthermore, the electromotive force is also affected by flow speed as seen in Fig. 3(a). Based on these results, a theoretical curve for output power P is calculated using the following equation:

$$P = \frac{R_L}{(r + R_L)^2} E^2. \quad (2)$$

Figure 3(d) compares the calculated P with measured values showing clear agreement. The maximum output under each flow speed is determined using this optimization.

The effect of the channel length on electricity generation was investigated next using several devices. The external load resistance for each device was optimized in advance for this investigation. Figure 4(a) shows the dependence of the electromotive force on flow speed. The electromotive forces from all devices with different channel lengths increase linearly with flow speed. The electromotive force per unit channel area is obtained after normalization [Fig. 4(b)] with a gradient of 0.0025 [$(\mu\text{V}/\text{mm}^2)/(\text{mm}/\text{s})$], which is the maximum output performance of this experimental design. Similarly, the maximum output power is obtained by fitting a quadratic function using Ohm's law. When DI water is used, the maximum performance of the flow-

induced electricity per unit area is determined by the flow speed. The results above clearly show that the generated electromotive force is proportional to both the channel area (contact area between graphene and water) and flow speed of water, indicating that the electric-field gradient in graphene changes linearly along the flow direction.

Several reports on electricity generation by liquid flow on carbon have focused on the role of electrolytes,^{3,26} explaining this phenomenon using a coulombic transfer model. However, our results here demonstrate that DI water flow can also generate electricity over graphene, indicating that a strong contribution of specific ions from the electrolyte solution is not the correct mechanism. This form of electricity generation probably requires either a polar liquid or an ionized solution. Likely, the ions in electrolyte solutions from previous experiments merely enhanced the output performance. Furthermore, other reports have proposed momentum transfer theory as a possible mechanism,⁸ where molecules from the flowing liquid medium transfer their momentum to the graphene phonons, inducing carrier motion via phonon-carrier interactions. In this case, the polarity of the generated voltage should depend on the type of charge carrier. Metallic materials generate high potential on the downstream side, while the p-type semiconductor does the opposite.²⁷ The results from this experiment including other reports³ show that the electrical current and liquid flow are always in the same direction when bulk graphene is used. Since this form of electricity generation is observed only from bulk graphene, further investigations are required to explain this phenomenon by momentum transfer theory. This suggests that both the coulombic transfer model and the momentum transfer theory are limited

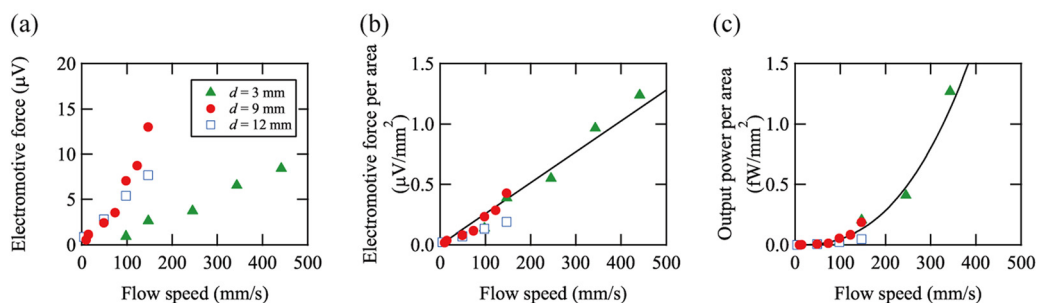


FIG. 4. (a) Dependence of the generated voltage on the channel length. (b) Normalized electromotive force. The solid line is linear fitting. The gradient of the fitting is 0.0025 [$(\mu\text{V}/\text{mm}^2)/(\text{mm}/\text{s})$]. (c) Normalized output power. The solid curve is fitted by the quadratic function.

to specific conditions of electricity generation from the graphene-water interface.

The formation of a continuous potential gradient in parallel to the flow direction still needs to be explained. This condition implies that there should be a difference between upstream and downstream of water flow.^{28–30} Streaming potential may not be appropriate to explain this phenomenon. This theory explains potential formation in a solution under the precondition that a fixed layer as a part of the electrical double layer exists. The properties of the channel walls except surface charge are not considered. Here, the capacitance charge/discharge model is applicable in terms of imbalance along the flow direction. However, while water flow is laminar in a typical macroscopic channel, the flow state is poorly understood at the microscopic scale by the experimental study, especially near the channel walls, where the electric effects of graphene cannot be accounted for using classical models. Therefore, future work should consider experimental differentiation between different states of the upstream and downstream flow in microchannels. This step will provide the key parameters to help solve the mechanism of electricity generation by liquid flow on carbon materials.

In conclusion, this work has quantified the output performance of electricity generation from the interface between graphene and flowing water. The results reveal that the generation of electromotive force is proportional to both the flow speed of water and the contact area, indicating the formation of a continuous potential gradient. In addition, the maximum performance of the electricity generation per unit area in the current setup is $0.0025 [(\mu\text{V}/\text{mm}^2)/(\text{mm}/\text{s})]$.

This work was supported by KAKENHI Grant No. 18K04880 and the Nanotechnology Platform Japan Program. The authors thank M. Nemoto for providing technical support for the spectroscopy measurement. They also acknowledge vitally important encouragement and support made through the University of Washington—Tohoku University: Academic Open Space (UW-TU: AOS).

DATA AVAILABILITY

The data that support the findings of this study are available from the corresponding author upon reasonable request.

REFERENCES

- ¹G. Xue, Y. Xu, T. Ding, J. Li, J. Yin, W. Fei, Y. Cao, J. Yu, L. Yuan, L. Gong, J. Chen, S. Deng, J. Zhou, and W. Guo, *Nat. Nanotechnol.* **12**, 317 (2017).
- ²J. Yin, Z. Zhang, X. Li, J. Yu, J. Zhou, Y. Chen, and W. Guo, *Nat. Commun.* **5**, 3582 (2014).
- ³S. S. Kwak, S. Lin, J. H. Lee, H. Ryu, T. Y. Kim, H. Zhong, H. Chen, and S.-W. Kim, *ACS Nano* **10**, 7297 (2016).
- ⁴T. Okada, G. Kalita, M. Tanemura, I. Yamashita, M. Meyyappan, and S. Samukawa, *Appl. Phys. Lett.* **112**, 023902 (2018).
- ⁵J. Yin, Z. Zhang, X. Li, J. Zhou, and W. Guo, *Nano Lett.* **12**, 1736 (2012).
- ⁶T. Okada, G. Kalita, M. Tanemura, I. Yamashita, M. Meyyappan, and S. Samukawa, *Adv. Eng. Mater.* **20**, 1800387 (2018).
- ⁷T. Okada, G. Kalita, M. Tanemura, I. Yamashita, F. S. Ouchi, M. Meyyappan, and S. Samukawa, *Results Phys.* **12**, 1291 (2019).
- ⁸P. Král and M. Shapiro, *Phys. Rev. Lett.* **86**, 131 (2001).
- ⁹S. Ghosh, *Science* **299**, 1042 (2003).
- ¹⁰B. N. J. Persson, U. Tartaglino, E. Tosatti, and H. Ueba, *Phys. Rev. B* **69**, 235410 (2004).
- ¹¹P. Dhiman, F. Yavari, X. Mi, H. Gullapalli, Y. Shi, P. M. Ajayan, and N. Koratkar, *Nano Lett.* **11**, 3123 (2011).
- ¹²Q. Yuan and Y.-P. Zhao, *J. Am. Chem. Soc.* **131**, 6374 (2009).
- ¹³J. Yin, X. Li, J. Yu, Z. Zhang, J. Zhou, and W. Guo, *Nat. Nanotechnol.* **9**, 378 (2014).
- ¹⁴A. E. Cohen, *Science* **300**, 1235 (2003).
- ¹⁵D. R. Kim, C. H. Lee, and X. Zheng, *Nano Lett.* **9**, 1984 (2009).
- ¹⁶F. H. J. van der Heyden, D. J. Bonthuis, D. Stein, C. Meyer, and C. Dekker, *Nano Lett.* **6**, 2232 (2006).
- ¹⁷F. H. J. van der Heyden, D. Stein, and C. Dekker, *Phys. Rev. Lett.* **95**, 116104 (2005).
- ¹⁸Z. L. Wang, T. Jiang, and L. Xu, *Nano Energy* **39**, 9 (2017).
- ¹⁹M.-L. Seol, J.-W. Han, D.-I. Moon, K. J. Yoon, C. S. Hwang, and M. Meyyappan, *Nano Energy* **44**, 82 (2018).
- ²⁰Z.-H. Lin, G. Cheng, S. Lee, K. C. Pradel, and Z. L. Wang, *Adv. Mater.* **26**, 4690 (2014).
- ²¹Y. Zi and Z. L. Wang, *APL Mater.* **5**, 074103 (2017).
- ²²W. Kim, T. Okada, H.-W. Park, J. Kim, S. Kim, S.-W. Kim, S. Samukawa, and D. Choi, *J. Mater. Chem. A* **7**, 25066 (2019).
- ²³S. Sharma, G. Kalita, R. Hirano, S. M. Shinde, R. Papon, H. Ohtani, and M. Tanemura, *Carbon* **72**, 66 (2014).
- ²⁴M. S. Rosmi, S. M. Shinde, N. D. A. Rahman, A. Thangaraja, S. Sharma, K. P. Sharma, Y. Yaakob, R. K. Vishwakarma, S. A. Bakar, G. Kalita, H. Ohtani, and M. Tanemura, *Mater. Res. Bull.* **83**, 573 (2016).
- ²⁵A. C. Ferrari, J. C. Meyer, V. Scardaci, C. Casiraghi, M. Lazzeri, F. Mauri, S. Piscanec, D. Jiang, K. S. Novoselov, S. Roth, and A. K. Geim, *Phys. Rev. Lett.* **97**, 187401 (2006).
- ²⁶X. Li, C. Shen, Q. Wang, C. M. Luk, B. Li, J. Yin, S. P. Lau, and W. Guo, *Nano Energy* **32**, 125 (2017).
- ²⁷J. Pei, J. Huang, Z. Huang, and K. Liu, *Sustainable Energy Fuels* **3**, 599 (2019).
- ²⁸Y. Xu, P. Chen, J. Zhang, S. Xie, F. Wan, J. Deng, X. Cheng, Y. Hu, M. Liao, B. Wang, X. Sun, and H. Peng, *Angew. Chem., Int. Ed.* **56**, 12940 (2017).
- ²⁹A. K. M. Newaz, D. A. Markov, D. Prasai, and K. I. Bolotin, *Nano Lett.* **12**, 2931 (2012).
- ³⁰Z. Zhuhua, X. Li, J. Yin, Y. Xu, W. Fei, M. Xue, Q. Wang, J. Zhou, and W. Guo, *Nat. Nanotechnol.* **13**, 1109 (2018).